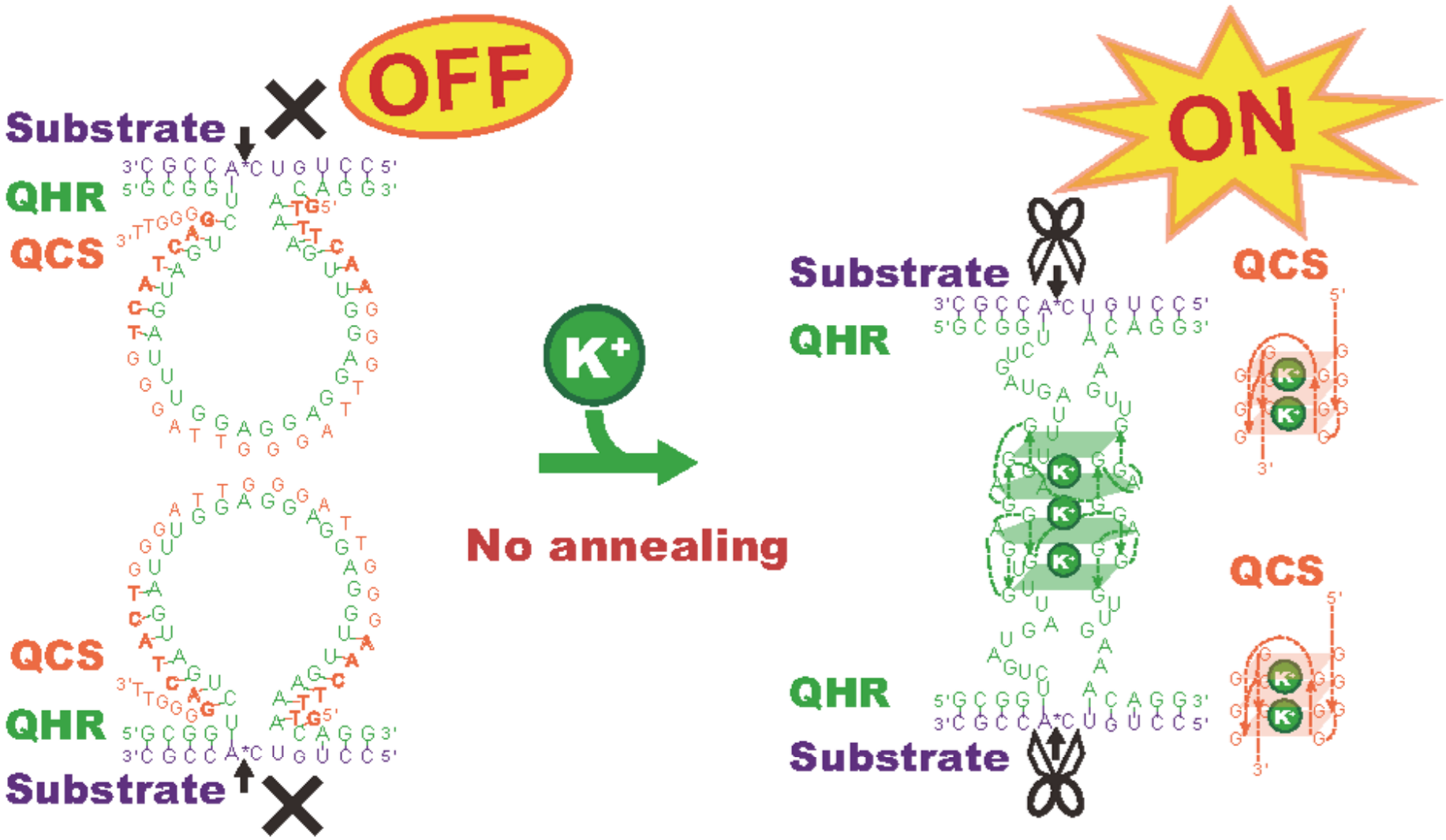

Graphical abstract

K^+-responsive off-to-on switching of hammerhead ribozyme through dual G-quadruplex formation requiring no heating and cooling treatment

Yudai Yamaoki[a, b], Takashi Nagata[a, b], Tsukasa Mashima[a, b], and Masato Katahira*[, a, b]

[a] Institute of Advanced Energy and [b]Graduate School of Energy Science, Kyoto University, Gokasho, Uji, Kyoto 611-0011, Japan.

* Corresponding author. Address: Institute of Advanced Energy, Kyoto University, Gokasho, Uji, Kyoto 611-0011, Japan (M. Katahira).

E-mail addresses: katahira@iae.kyoto-u.ac.jp (M. Katahira).

Keywords:

G-Quadruplex

Structural transition

RNA structure

Switching of activity

Ribozyme

Potassium

ABSTRACT

Functional RNAs that switch their activities in response to K^+ may sense the intracellular (100 mM) and extracellular (5 mM) K^+ concentrations and regulate their functions accordingly. Previously, we developed a quadruplex hammerhead ribozyme (QHR) whose conformational change, from a duplex to a G-quadruplex, triggered by K^+ results in expression of the activity. However, this QHR required heating

and cooling treatment (annealing) to induce the K^+-responsive conformational change and activity. Here, we developed a new quadruplex hammerhead ribozyme (QHR) system that does not require annealing to induce the K^+-responsive conformational change and activity. This system is composed of QHR and a G-quadruplex-forming complementary DNA strand (QCS). In the absence of K^+, QCS formed a duplex with QHR, which suppressed the residual activity. Upon elevation of the K^+ concentration, QCS dissociated from QHR was trapped in a G-quadruplex, and then QHR could form a G-quadruplex and exerted the activity. The 11.6-fold higher activity was induced by K^+ with an EC_{50} value of 23 mM, but not by Na^+, which is desirable when the activity switching between the intra-/extracellular environment is aimed at. This is the first report of the activation of functional RNA through a 'dual G-quadruplex formation system'.

1. Introduction

Guanine (G)-rich nucleic acids reportedly fold into a compact G-quadruplex structure in response to K^+, but in the absence of K^+ the structure is elongated and single-stranded [1-4]. Thus, we recognized these nucleic acids as a conformational switch that can be turned 'ON' by using K^+ as a switching stimulator. The concentration of K^+ inside cells (about 100–150 mM) is much higher than that outside the cells (3.5–5.5 mM). Therefore, in principle, such G-rich nucleic acids should dramatically change their conformations when they are delivered from an extracellular to an intracellular environment. We hypothesized that if we combined such G-rich RNAs with functional RNAs such as ribozymes and aptamers, we would be able to obtain novel ribozymes and aptamers that sense differences in the K^+ concentration between cellular environments and thereby exert their activities.

In the previous study, we determined the G-quadruplex structure of 5′-r(GGAGGAGGAGGA)-3′ (R12) in the presence of K^+ [5,6]. R12 forms a parallel G-quadruplex conformation that comprises G:G:G:G tetrad and G:(A):G:G:(A):G hexad planes. The R12 quadruplex becomes a stable dimer through stacking interaction between the hexads of the G-quadruplex. However, in the absence of K^+, R12 takes on an elongated single-stranded form and does not form a particular structure. We have also shown that R11, which lacks the terminal adenine residue of R12, has similar structural characteristics both in the presence and absence of K^+ [7].

In a hammerhead ribozyme (HR), two domains of the catalytic core, the 5′-HR domain (5′-GCGGUCUGAUGA-3′) and the 3′-HR domain (5′-GAAACAGG-3′), are connected by a central stem (Fig. S1). The two closely located domains exert the ribozyme activity independently of K^+ [8,9]. We have previously introduced R11 into a hammerhead ribozyme (HR) and developed an artificially designed ribozyme, Quadruplex Hammerhead Ribozyme (QHR) (Table S1) [7]. In QHR, the stem of HR is replaced by R11 and uridine-linkers, by which the two domains are linked. QHR switches its ribozyme activity 'ON' in response to K^+ (Scheme S1A, B). In the absence of K^+, the 5′-HR and 3′-HR domains are located rather far apart because R11 takes on the elongated single-stranded form (Scheme S1A), but in the presence of K^+ they are brought into close proximity due to the formation of the compact R11 G-quadruplex, by which QHR exerts activity (Scheme S1B).

QHR exerts higher activity in the presence of K^+ than its absence [7] as we have hypothesized. Unexpectedly, however, QHR showed unexpected ribozyme activity even in the absence of K^+, namely residual activity. We speculated that in the absence of K^+, the R11 region of QHR takes on a flexible single-stranded form and that the unexpected active core structure of QHR is partially and/or transiently formed [7]. We have introduced RNA that is partially complementary to QHR (named CS, Table S1). In the presence of CS, CS forms a duplex with QHR in the absence of K^+, which keeps the 5′- and 3′-HR regions of the QHR apart from each other (Scheme S1D). Accordingly, the formation of a partial and/or transient structure of the active core was inhibited, resulting in suppression of the residual activity of QHR in the absence of K^+ [10]. In the presence of K^+, R11 of QHR forms a G-quadruplex and the active core structure is restored, resulting in effective cleavage of the substrate (Scheme S1E). Thus, the introduction of CS successfully suppressed the residual activity of QHR in the absence of K^+, while in the presence of K^+ the activity is fully exerted. In the presence of CS, the switching efficiency of QHR, which can be defined as the ratio of the activity between in the absence and presence of K^+, drastically increased. In spite of these improvements, however, this system required annealing treatment (heating and cooling processes) for the K^+-responsive conformational change from the inactive duplex form to the active G-quadruplex form (Scheme S1D, E). The conformational change did not occur if the annealing treatment was not performed (Scheme S1F). In the present study, in order to apply QHR to living cellular environments, we developed a new QHR system, in which the residual activity is suppressed (left of Scheme 1 and S1H) and transition to the active form is induced just by the addition of K^+, namely without the annealing treatment

(right of Scheme 1 and S1I). This newly constructed QHR system that makes use of G-quadruplex-forming complementary DNA strand (QCS) could be a prototype for the development of such switching-molecules that can be applied to living cellular environments.

2. Materials and methods

2.1. Oligonucleotides

The quadruplex hammerhead ribozyme (QHR) (5'-r(GCGGUCUGAUGAUUUGGAGGAGGAGGUUGAAACAGG)-3'), complementary RNA strand (CS) (5'-r(CUCCUUUUCAUC)-3'), G-quadruplex-forming complementary DNA strand (QCS) (5'-d(GTTTCAAGGGTTAGGGTTAGGGTCATCAGGGGTT)-3'), and 5'-end fluorescein-5-isothiocyanate (FITC)-labelled substrate RNA (5'-CCUGUCACCGC-3') were synthesized, purified, and desalted by FASMAC Co., Ltd. (Kanagawa, Japan).

2.2. Cleavage reactions and kinetic measurements

QHR was dissolved either alone or with a complementary nucleic acid (CS or QCS) in ca. 70 mM Tris-HCl buffer (pH 8.0), and then incubated at 95 °C for 5 min. It was then cooled to 30 °C in 60 min, followed by incubation at 25 °C for 30 min. QHR (10 μM) either alone or with a complementary nucleic acid (CS or QCS, 30 μM) dissolved in 50 mM Tris-HCl buffer (pH 8.0), 50 mM $MgCl_2$, and either 0 or 100 mM NaCl with various concentrations of KCl was incubated at 25 °C for 40 min. The cleavage reaction was initiated by addition of the 5'-end FITC-labeled substrate RNA (1 μM). The temperature was kept at 25 °C during the reaction using a thermal cycler (TAKARA BIO, Japan). A small aliquot was taken from the solution at each time point and the reaction was terminated by the addition of EDTA (83 mM) and urea (7.5 M). These small aliquots were applied to a denaturing 20 % polyacrylamide gel, by which uncleaved and cleaved substrates were isolated during electrophoresis. The amounts of FITC-labeled substrates were determined from the intensities of the fluorescence bands using a Pharos FX^{TM} Molecular Imager (BIO-RAD).

The cleavage percentage of the substrate was defined as the amount of cleaved substrate divided by the sum of the amounts of uncleaved and cleaved substrates. The first-order rate constant, k_{obs}, was determined

by curve fitting of the time-course experiment data to the equation: P (t) = P_{max} - (P_{max} - P_0) exp (-k_{obs} t), where P (t) is the cleavage percentage at time t, P_{max} the cleavage percentage at infinite time, and P_0 the extrapolated cleavage percentage at t = 0 [7,11]. Error bars are standard deviation calculated for three trials.

2.3. K^+-concentration dependence of the ribozyme activity of the QHR-QCS system

The K^+ dependence of the activity of the QHR-QCS system was evaluated. Various amounts of KCl were added to samples containing the pre-formed QHR-QCS duplex. Then the activity of QHR was examined at each K^+ concentration without the annealing treatment. The fraction of the active form of QHR (f_{active}) was deduced using equation (1) on the assumption that QHR was fully activated at 300 mM KCl.

$$f_{\mathrm{active}} = \frac{k_{\mathrm{obs}}^{[\mathrm{K^+}]}}{k_{\mathrm{obs}}^{[300\ \mathrm{mM}]}} \qquad (1)$$

The half maximal effective concentration of KCl (EC_{50}) for activation of QHR was obtained with equation (2).

$$f_{\mathrm{active}} = \frac{[\mathrm{K^+}]}{\mathrm{EC}_{50}+[\mathrm{K^+}]} \qquad (2)$$

2.4. Circular dichroism (CD) measurements

QHR (14 μM) and QCS (14 μM) were dissolved in 5 mM sodium phosphate buffer (pH 6.5) and 5 mM $MgCl_2$, and then incubated at 95 °C for 5 min. The mixture was then cooled to 30 °C in 60 min, followed by incubation at 25 °C for 30 min using a thermal cycler. Subsequently, KCl was added to the sample solution to the final concentration of either 0 or 100 mM. CD spectra were recorded at 5 °C with a cell of 1 mm path length using a J-720 spectropolarimeter (JASCO, Tokyo, Japan).

2.5. Nuclear magnetic resonance (NMR) measurements

QHR and QCS were dissolved at the final concentration of 70 μM in 5 mM sodium phosphate buffer (pH 6.5), containing 5 mM $MgCl_2$. Each sample solution was incubated at 95 °C for 5 min and cooled to 30 °C in 60 min, and then incubated at 25 °C for 30 min using a thermal cycler. Subsequently, KCl was

added to the sample solution to the final concentration of either 0 or 100 mM. NMR spectra were recorded at 25 °C using a Bruker BioSpin DRX600 and AVANCE III HD 600 spectrometer equipped with a cryogenic probe with a Z-gradient. 2,2-dimethylsilapentane-5-sulfonic acid (DSS) was used as an internal chemical shift reference.

3. Results and discussion

3.1. Construction of a G-Quadruplex-forming Complementary DNA Strand (QCS) for development of a new QHR system requiring no annealing treatment

With the coexistence of CS, the structural change of QHR from a duplex to a G-quadruplex occurs only when K^+ is added and at the same time annealing treatment is performed (Scheme S1E). The QHR-CS duplex dissociates during the heating process. Here, the G-quadruplex of QHR has a higher melting temperature than that of the QHR-CS duplex in the presence of K^+. Therefore, the G-quadruplex of QHR is preferred over the QHR-CS duplex in and after the cooling process. Thus, in the presence of CS, QHR efficiently induces the activity in response to K^+ with annealing treatment. However, in the presence of K^+ and without heating, although it may be possible for the QHR-CS duplex to transiently dissociate, reformation of the QHR-CS duplex is efficient and results in inhibition of the structural change of QHR to the G-quadruplex. Therefore, for activation that does not require the annealing, it seems necessary to suppress the reformation of the duplex between QHR and CS when K^+ is added. In this study, we attempted to trap CS in G-quadruplex upon dissociation from QHR in the presence of K^+, which should inhibit the reformation of the duplex between QHR and CS. We chose a human telomeric DNA, $(TTAGGG)_4TT$, which was reported to form a G-quadruplex in the presence of K^+ [12-14], as a template of such a new class of CS. Two of the four TTA sequences of this DNA sequence were replaced with complementary sequences as to QHR, the resultant DNA being named the G-quadruplex-forming complementary DNA strand (QCS, 5'-d(GTTTCAAGGGTTAGGGTTAGGGTCATCAGGGGTT)-3', Table S1). In the absence of K^+, the formation of the duplex between QHR and QCS is expected to suppress the residual activity of QHR (left of Scheme 1 and S1H). On the other hand, QCS that transiently dissociates from QHR is expected to form a G-quadruplex in the presence of K^+, losing its ability to re-form the duplex with QHR (right of Scheme 1 and S1I). Concurrently, QHR is expected to fold into a

G-quadruplex and exerts its activity just with the addition of K^+, namely without annealing treatment (right of Scheme 1 and S1I).

3.2. Ribozyme activity assaying of QHR with the coexistence of QCS

QHR alone or with complementary nucleic acids (CS or QCS) either in the absence or presence of 100 mM K^+ was incubated at 25 °C for 40 min. The RNA cleavage reaction of QHR was initiated by addition of 5'-end FITC-labeled substrate RNA to a final concentration of 1 μM. The ribozyme activities of the QHR in the absence and presence of 100 mM K^+ were determined by polyacrylamide gel electrophoresis (Fig. 1A). First-order rate constants were obtained from these results [7,10] (bottom of Fig. 1C). The ratio of the first-order rate constants under either 0 or 100 mM KCl conditions, k_{obs}^{100mM} / k_{obs}^{0mM} (switching efficiency), were calculated and are shown in top of Fig. 1C. In the absence of neither CS nor QCS, the first-order rate constant of QHR in the absence of K^+ (k_{obs}^{0mM}) was 2.8 x 10^{-2} s^{-1}, while that in the presence of 100 mM K^+ (k_{obs}^{100mM}) was 4.4 x 10^{-2} s^{-1} (bottom of Fig. 1C). In the case of QHR alone, the activity was indeed enhanced in response to K^+, a switching efficiency of ca. 1.6-fold (top of Fig. 1C, "QHR"). However, in the absence of neither CS nor QCS, the QHR exhibited non-negligible residual activity even in the absence of K^+ (bottom of Fig. 1C, "QHR"). On the other hand, with the coexistence of CS, k_{obs}^{0mM} = 4.8 x 10^{-3} s^{-1} and k_{obs}^{100mM} = 5.1 x 10^{-3} s^{-1} were obtained (bottom of Fig. 1C). The residual activity of the QHR in the presence of CS, was suppressed to approximately 17 % of the level for QHR alone (compare "QHR" and "QHR+CS" in bottom of Fig. 1C). However, addition of KCl alone failed to induce the activity of QHR with CS ("QHR+QCS" in bottom and top of Fig. 1C). In the case of QHR with CS, annealing treatment is needed to switch "ON" the activity along with the addition of KCl. In fact, when annealing is applied after the addition of K^+, switching efficiency of 21.4 was achieved for QHR in the presence of CS [10].

In the case of the QHR system where QCS coexists, k_{obs}^{0mM} = 2.6 x 10^{-3} s^{-1} and k_{obs}^{100mM} = 3.1 x 10^{-2} s^{-1} were obtained (bottom of Fig. 1C, "QHR+QCS"). The introduction of QCS significantly suppressed the residual activity, which was 9 % of the level for QHR alone. Importantly, the activity enhancement occurred in response to just K^+, annealing not being required (bottom and top of Fig. 1C). Thus, the introduction of QCS resulted in suppression of the residual activity and the K^+-responsive activity enhancement without annealing treatment at the same time. As a result of the successful suppression of

residual activity, the switching efficiency increased to 11.6 (top of Fig. 1C). The switching efficiency of QHR alone was 1.6 and almost no enhancement (1.1) was observed for the QHR with CS when annealing was not applied (top of Fig. 1C). Thus, the great improvement of the switching efficiency of QHR was achieved as a result of the introduction of QCS even without annealing treatment.

3.3. K^+-responsive conformational change of QHR and QCS from a duplex to a G-quadruplex examined by NMR and CD

The duplex to G-quadruplex structural transition of QHR and QCS was examined by NMR. In the absence of K^+, the observation of imino proton resonances at 11.6 - 12.6 ppm and 13.0 - 14.4 ppm (Fig. 2A) indicates the formation of G:C and A:T (A:U) base pairs in the duplex, respectively, which is consistent with the design scheme (left of Scheme 1 and S1H). In the presence of K^+, the intensity of these resonances drastically decreased. Alternatively, new resonances appeared at 10.8 – 12.0 ppm (Fig. 2B), which indicates the formation of tetrads of the G-quadruplexes. These findings confirm the duplex to G-quadruplex transition, which is consistent with the design scheme (right of Scheme 1 and S1I). The CD spectral change of QHR and QCS with increasing K^+ concentration also supports the formation of the G-quadruplexes (Fig. S2). The duplex to G-quadruplex structural transition for a QHR-QCS system was supported by native PAGE analysis as well (Fig. S3 and S4).

3.4. K^+ and Na^+ dependence of the ribozyme activity of the QHR-QCS system

The activity of the QHR-QCS system was examined at each K^+ concentration without the annealing treatment. With an increase in the K^+ concentration, the activity of QHR increased (Fig. 3). The activity almost reached a plateau at 300 mM KCl. Therefore, the fraction of the active form of QHR (f_{active}) was deduced on the assumption that QHR was fully activated at 300 mM KCl. The half maximal effective concentration of KCl (EC_{50}) was determined to be 23.0 mM.

Moreover, the activity of the QHR-QCS system turned out to be very low in the presence of 100 mM Na^+, the value of $k_{obs}^{100mM\ NaCl}$ being just 15 % of the first-order rate constant at 100 mM K^+ ($k_{obs}^{100mM\ KCl}$ = 3.1 x 10^{-2} s^{-1}) (Fig. S5).

3.5. Relationship with previous studies and the possibility of application

Switching of the ribozyme and DNAzyme activity through duplex-quadruplex structural transition with K^+, Na^+, ATP, oligo DNA, and proteins has been reported by several groups including ours [10,15-21]. To the best of our knowledge, however, our QHR-QCS system is the first one that involves switching of the ribozyme activity through duplex - G-quadruplex transition in response to K^+ without annealing treatment. This system should be appropriate for cellular application when annealing treatment cannot be carried out. Furthermore the activity was induced by K^+ with an EC_{50} value of 23 mM, but not by Na^+. Since the intracellular K^+ concentration is ca. 100 mM, while the extracellular K^+ concentration is ca. 5 mM, the QHR-QCS system should be inactive outside a cell, but once it enters the cell, its activity is expected to be induced autonomously. When a drug delivery system (DDS) is considered, this QHR system may work as a way to release functional RNAs that target intracellular molecules from carriers. Thus the system may be useful to develop a new efficient DDS.

Our method can be applied to other functional nucleic acids such as an RNA aptamer, DNA aptamer, and DNAzyme. There could be situations in which an RNA aptamer that targets either a certain protein or a small molecule should be silent outside the cell to avoid side effects and should function only inside the cell. Our method involving dual G-quadruplex formation has potential to afford an RNA aptamer with these required properties.

Acknowledgments

We thank Professors T. Morii and E. Nakata of Kyoto University for their technical support with the fluorescence gel imaging systems. This work was supported by JSPS KAKENHI 25291013, 26104520, 26650014 and 15H01256 to M.K., 15H01634 and 26440026 to T.N., and 15H00813 to T.M., and a JSPS Research Fellow Program grant to Y.Y.

References

[1] S. Burge, G.N. Parkinson, P. Hazel, A.K. Todd, S. Neidle, Quadruplex DNA: sequence, topology and structure, Nucleic Acids Res. 34 (2006) 5402-5415.

[2] D.E. Gilbert, J. Feigon, Multistranded DNA structures, Curr. Opin. Struct. Biol. 9 (1999) 305-314.

[3] A.N. Lane, J.B. Chaires, R.D. Gray, J.O. Trent, Stability and kinetics of G-quadruplex structures, Nucleic Acids Res. 36 (2008) 5482-5515.

[4] A.T. Phan, V. Kuryavyi, D.J. Patel, DNA architecture: from G to Z, Curr. Opin. Struct. Biol. 16 (2006) 288-298.

[5] T. Mashima, A. Matsugami, F. Nishikawa, S. Nishikawa, M. Katahira, Unique quadruplex structure and interaction of an RNA aptamer against bovine prion protein, Nucleic Acids Res. 37 (2009) 6249-6258.

[6] T. Mashima, F. Nishikawa, Y.O. Kamatari, H. Fujiwara, M. Saimura, T. Nagata, T. Kodaki, S. Nishikawa, K. Kuwata, M. Katahira, Anti-prion activity of an RNA aptamer and its structural basis, Nucleic Acids Res. 41 (2013) 1355-1362.

[7] T. Nagata, Y. Sakurai, Y. Hara, T. Mashima, T. Kodaki, M. Katahira, 'Intelligent' ribozyme whose activity is altered in response to K^+ as a result of quadruplex formation, FEBS J. 279 (2012) 1456-1463.

[8] K.J. Hertel, A. Pardi, O.C. Uhlenbeck, M. Koizumi, E. Ohtsuka, S. Uesugi, R. Cedergren, F. Eckstein, W.L. Gerlach, R. Hodgson, Numbering system for the hammerhead, Nucleic Acids Res. 20 (1992) 3252.

[9] O.C. Uhlenbeck, A small catalytic oligoribonucleotide, Nature 328 (1987) 596-600.

[10] Y. Yamaoki, T. Mashima, T. Nagata, M. Katahira, Boosting of activity enhancement of K^+-responsive quadruplex hammerhead ribozyme, Chem. Commun. (Camb.) 51 (2015) 5898-5901.

[11] T. Sakamoto, M.H. Kim, Y. Kurihara, N. Sasaki, T. Noguchi, M. Katahira, S. Uesugi, Properties of a hammerhead ribozyme with deletion of stem II, J. Biochem. 121 (1997) 288-294.

[12] J. Dai, M. Carver, C. Punchihewa, R.A. Jones, D. Yang, Structure of the Hybrid-2 type intramolecular human telomeric G-quadruplex in K^+ solution: insights into structure polymorphism of the human telomeric sequence, Nucleic Acids Res. 35 (2007) 4927-4940.

[13] K.N. Luu, A.T. Phan, V. Kuryavyi, L. Lacroix, D.J. Patel, Structure of the human telomere in K^+ solution: an intramolecular (3 + 1) G-quadruplex scaffold, J. Am. Chem. Soc. 128 (2006) 9963-9970.

[14] A. Matsugami, Y. Xu, Y. Noguchi, H. Sugiyama, M. Katahira, Structure of a human telomeric

DNA sequence stabilized by 8-bromoguanosine substitutions, as determined by NMR in a K^+ solution, FEBS J. 274 (2007) 3545-3556.

[15] J.L. Neo, K. Kamaladasan, M. Uttamchandani, G-quadruplex based probes for visual detection and sensing, Curr. Pharm. Des. 18 (2012) 2048-2057.

[16] J.D. Beaudoin, J.P. Perreault, Potassium ions modulate a G-quadruplex-ribozyme's activity, RNA 14 (2008) 1018-1025.

[17] C. Teller, S. Shimron, I. Willner, Aptamer-DNAzyme hairpins for amplified biosensing, Anal. Chem. 81 (2009) 9114-9119.

[18] H. Sun, X. Li, Y. Li, L. Fan, H.B. Kraatz, A novel colorimetric potassium sensor based on the substitution of lead from G-quadruplex, Analyst 138 (2013) 856-862.

[19] Y. Zhao, H. Chen, F. Du, A. Yasmeen, J. Dong, X. Cui, Z. Tang, Signal amplification of glucosamine-6-phosphate based on ribozyme glmS, Biosens. Bioelectron. 62 (2014) 337-342.

[20] S. Bhadra, V. Codrea, A.D. Ellington, G-quadruplex-generating polymerase chain reaction for visual colorimetric detection of amplicons, Anal. Biochem. 445 (2014) 38-40.

[21] Y. Hu, F. Wang, C.H. Lu, J. Girsh, E. Golub, I. Willner, Switchable enzyme/DNAzyme cascades by the reconfiguration of DNA nanostructures, Chem. Eur. J. 20 (2014) 16203-16209.

Figure Legends

Scheme 1. The architecture and activation scheme of QHR with QCS system. The sequences of QHR (green), substrate RNA (purple), and QCS (orange) are shown. The residues of QCS that form base pairs with QHR are shown in bold. The cleavage site of the substrate RNA is indicated by a black arrow. The formation of the QHR-QCS duplex represses the residual activity of QHR (left). Addition of K^+ induces the formation of the G-quadruplex for both QHR and QCS, by which QHR exerts its activity (right). Here, annealing is not required for the activation.

Fig. 1. Activity assays of QHR systems. (A) Polyacrylamide gel electrophoresis of the products produced during the cleavage of the FITC-labeled substrate RNA with QHR+QCS. The reactions were performed either with 0 (top) or 100 mM KCl (bottom). (B) Time course of increasing cleavage product with

QHR+QCS either at 0 mM KCl (open circles, dashed line) or 100 mM KCl (filled circles, solid line). (C) Bottom, the first-order rate constants (k_{obs}) obtained by curve fitting of the time-course experiment results for the cleavage reaction. Bar graphs present k_{obs} for reactions performed either with 0 mM K^+ (k_{obs}^{0mM}, open boxes) or 100 mM K^+ (k_{obs}^{100mM}, filled boxes). Top, gray boxes present the ratios of the rate constants, $k_{obs}^{100mM} / k_{obs}^{0mM}$.

Fig. 2. NMR spectra of the mixture of QHR and QCS. QHR (70 μM) and QCS (70 μM) were dissolved in 5 mM sodium phosphate buffer (pH 6.5) containing 5 mM $MgCl_2$, and either 0 mM (A) or 100 mM (B) KCl at 25 °C.

Fig. 3. K^+-concentration dependence of the ribozyme activity of the QHR-QCS system. The fraction of the active form of QHR at each KCl concentration was deduced from the rate constants (k_{obs}) for the cleavage reaction. The solid line was drawn by the curve fitting with equation (2).

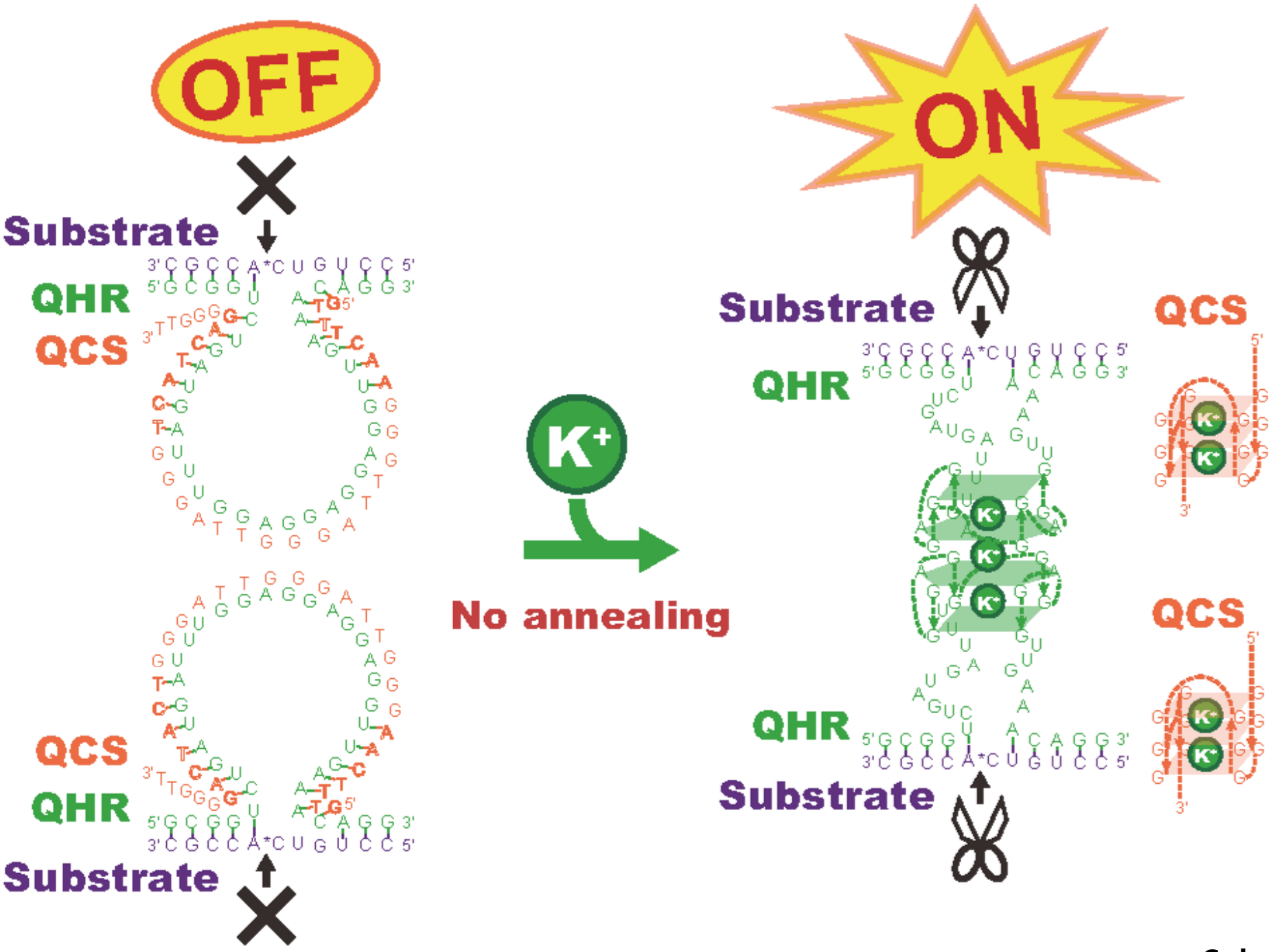
OFF
Substrate
QHR
QCS
QCS
QHR
Substrate
K+
No annealing
ON
Substrate
QHR
QCS
QCS
QHR
Substrate

Scheme 1

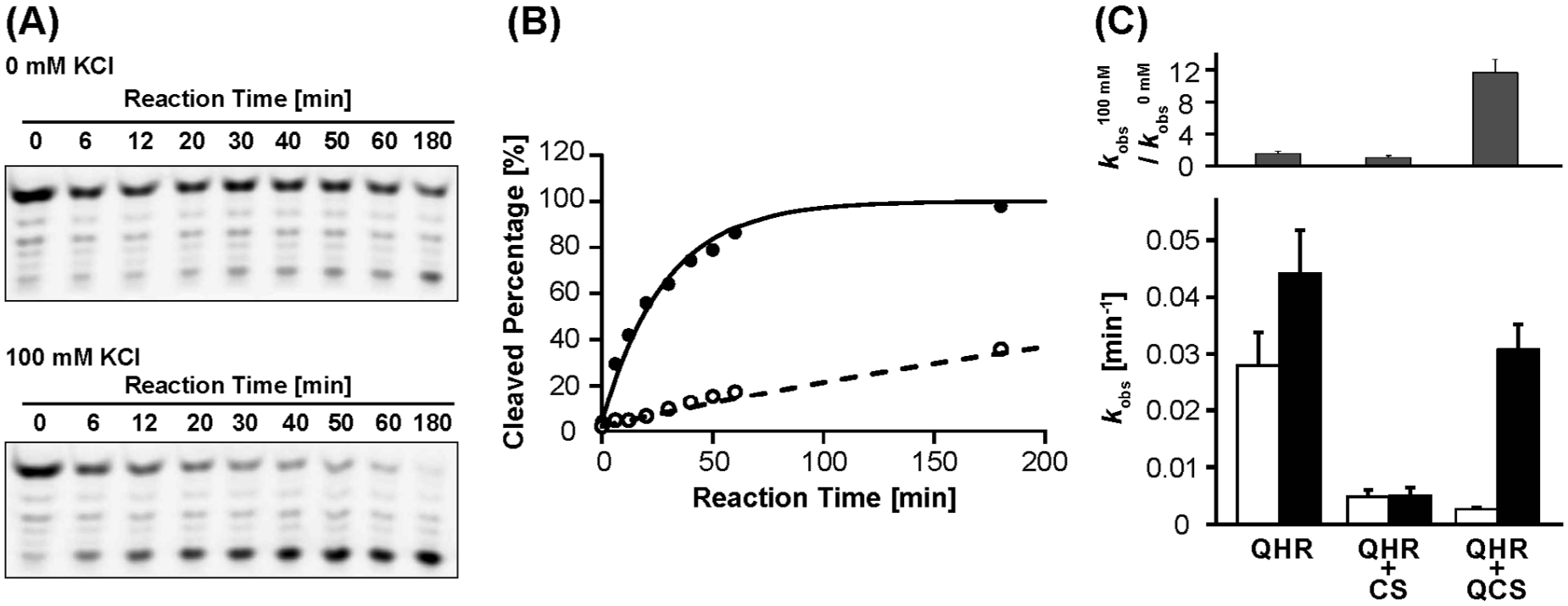
(A)
0 mM KCl
Reaction Time [min]
0 6 12 20 30 40 50 60 180
100 mM KCl
Reaction Time [min]
0 6 12 20 30 40 50 60 180
(B)
Cleaved Percentage [%]
120
100
80
60
40
20
0
0 50 100 150 200
Reaction Time [min]
(C)
$k_{obs}^{100\ mM} / k_{obs}^{0\ mM}$
12
8
4
0
k_{obs} [min^{-1}]
0.05
0.04
0.03
0.02
0.01
0
QHR
QHR + CS
QHR + QCS

Fig. 1

Fig. 2

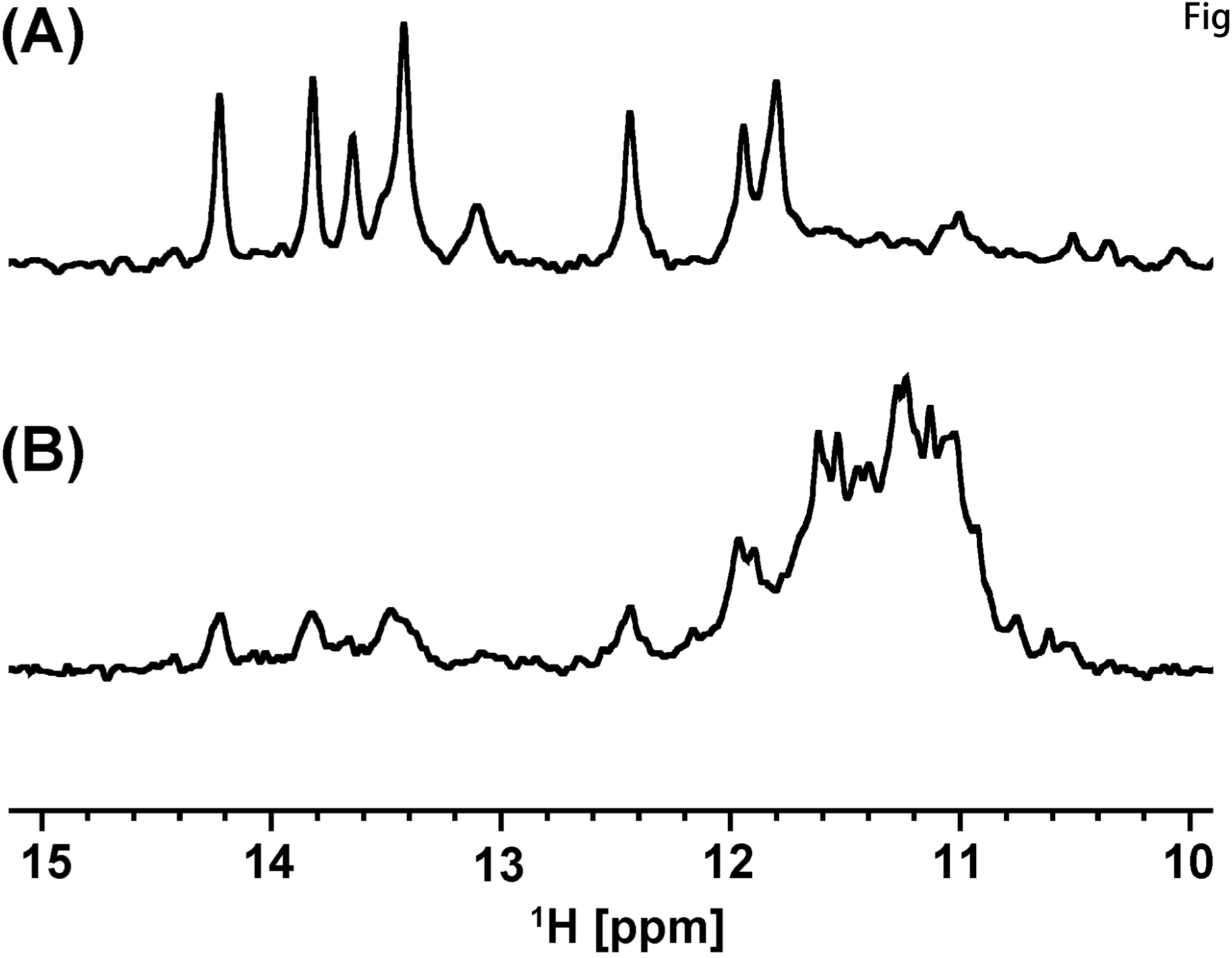

Fig. 3

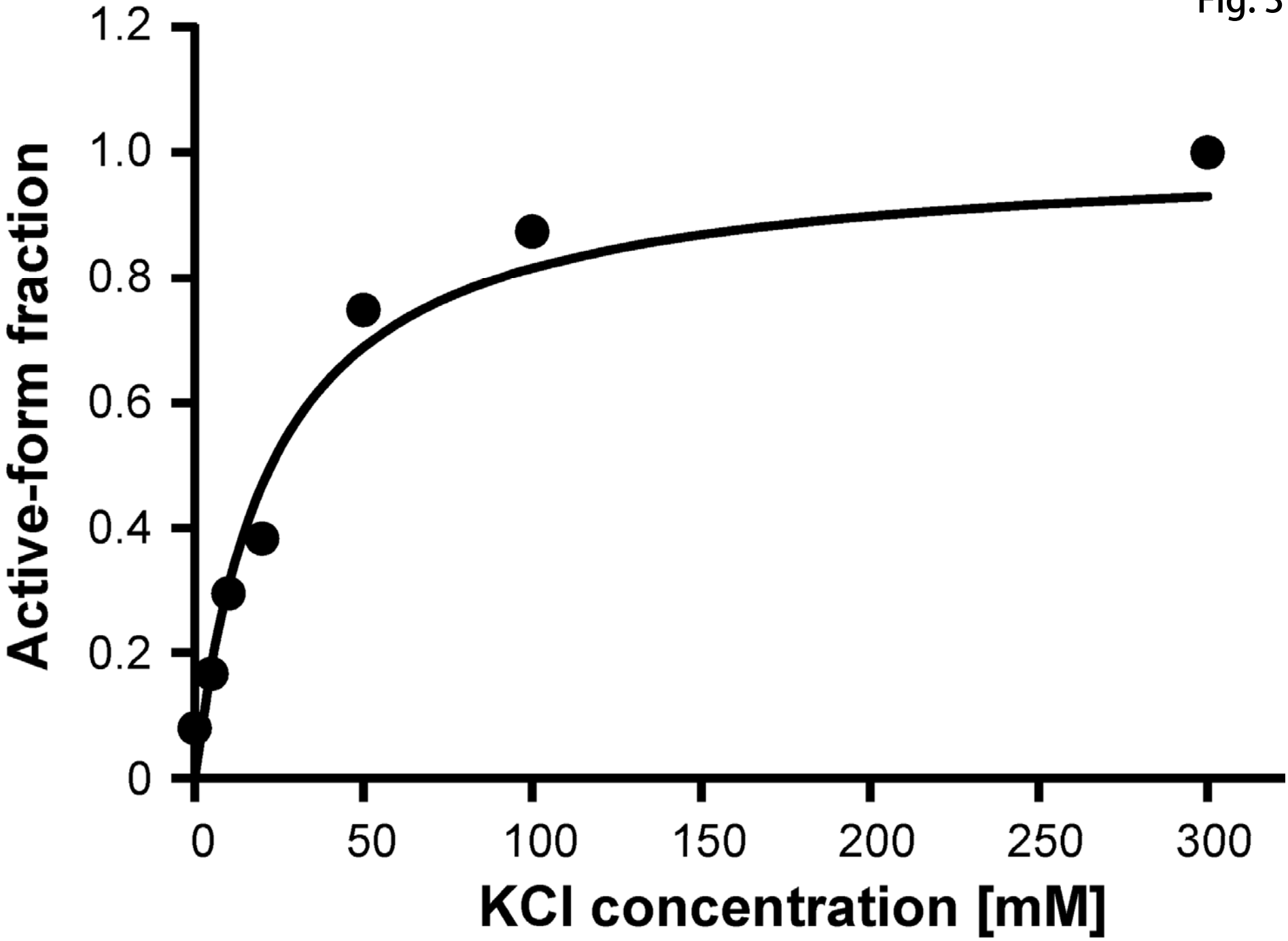
Active-form fraction
1.2
1.0
0.8
0.6
0.4
0.2
0
0
50
100
150
200
250
300
KCl concentration [mM]

Biochemical and Biophysical Research Communications

Supporting Information

K^+-responsive off-to-on switching of hammerhead ribozyme through dual G-quadruplex formation requiring no heating and cooling treatment

Yudai Yamaoki, Takashi Nagata, Tsukasa Mashima, and Masato Katahira*

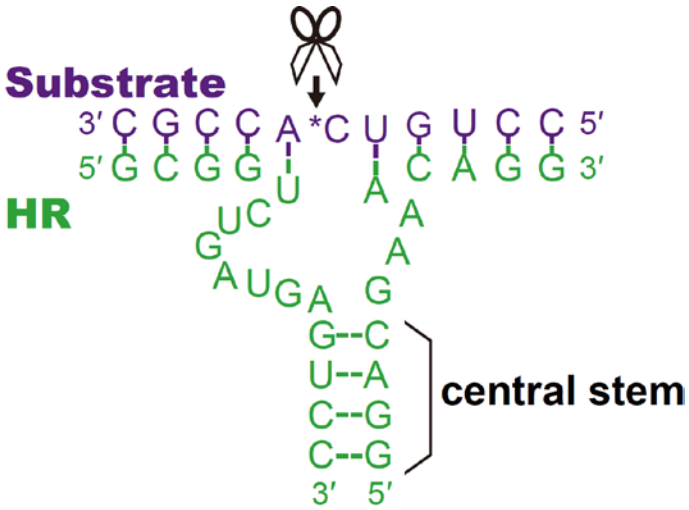

Fig. S1. The architecture of a hammerhead ribozyme (HR). The sequences of HR (green) and substrate RNA (purple) are shown. Base pairs are represented as a dotted line. The cleavage site of the substrate RNA is indicated by a black arrow. Two domains of the catalytic core, the 5′-HR domain (5′-GCGGUCUGAUGA-3′) and the 3′-HR domain (5′-GAAACAGG-3′), are connected by a central stem.

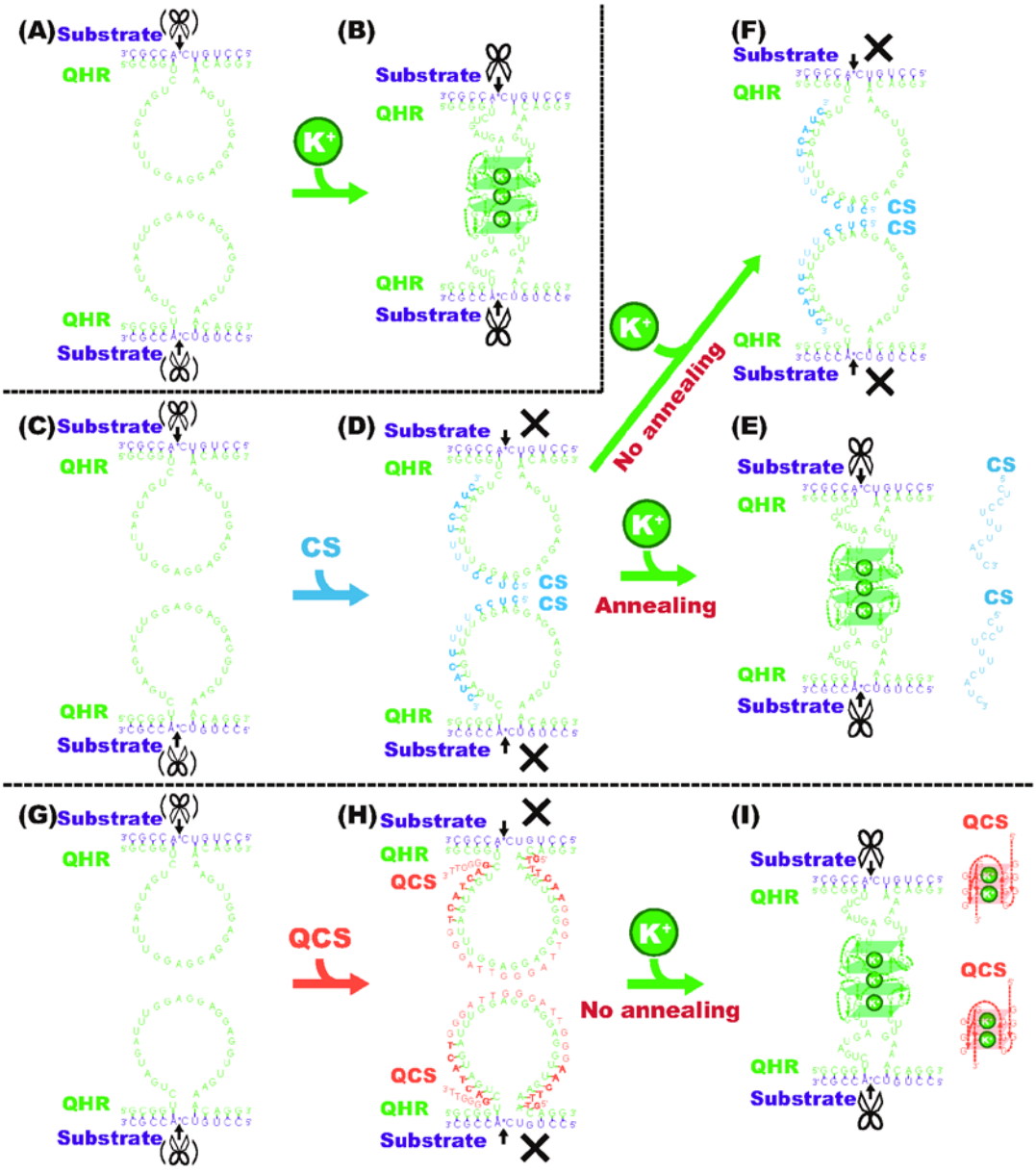

Scheme S1. The architecture and activation scheme of each QHR system. The sequences of QHR (green), substrate RNA (purple), CS (blue), and QCS (orange) are shown. The residues of either CS or QCS that form base pairs with QHR are shown in bold. The cleavage site of the substrate RNA is indicated by a black arrow. QHR shows residual activity even in the absence of K^+ (A, C, G). (A, B) QHR alone. QHR exerts RNA cleavage activity via G-quadruplex formation in response to K^+. (C-F) QHR with CS. The formation of the QHR-CS duplex represses the residual activity of QHR (D). Addition of K^+ followed by annealing results in activation of QHR (E). Addition of K^+ without annealing does not induce activation (F). (G-I) QHR with QCS. The formation of the QHR-QCS duplex represses the residual activity of QHR (H). Addition of K^+ induces the formation of the G-quadruplex for both QHR and QCS, by which QHR exerts its activity. Here, annealing is not required for the activation.

Table S1. The sequences of the quadruplex hammerhead ribozyme (QHR), complementary RNA strand (CS), and G-quadruplex-forming complementary DNA strand (QCS). The bases that form base pairs between QHR and CS are indicated by italic characters, and those between QHR and QCS are indicated by bold characters. The residues of R11 of QHR are indicated by underlines. The guanosine residues of QCS that form the tetrads of the G-quadruplex are indicated by underlines.

Name	Sequence
QHR	5′-r(GCGGU**CU*GAUGA***UUU*GGAG*GAGGAGG**UUGAAAC**AGG)-3′
CS	3′-r(*CUACU*UUU*CCUC*)-5′
QCS	3′-d(TTGGG**GACTACT**GGGATTGGGATTGGG**AACTTTG**)-5′

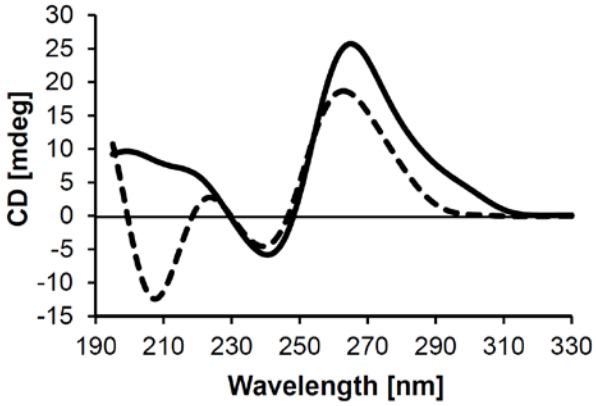

Fig. S2. CD spectra of a mixture of QHR and QCS. QHR (14 μM) and QCS (14 μM) were dissolved in 5 mM sodium phosphate buffer (pH 6.5) containing 5 mM $MgCl_2$, and either 0 mM (dashed line) or 100 mM (solid line) KCl at 5 °C. Addition of 100 mM K^+ resulted in an increase in the intensity of the positive band at around 260 nm, which suggests the formation of a parallel G-quadruplex [1,2]. This is consistent with the design scheme for the QHR-QCS system in which the R11 portion of QHR is expected to form a parallel G-quadruplex upon elevation of the K^+ concentration [3,4]. Additionally, a positive band appeared at around 295 nm when 100 mM K^+ was added. This suggests the formation of a hybrid-type mixed parallel/antiparallel-stranded G-quadruplex [5,6,9], which is also consistent with the design scheme in which QCS involving the sequences of human telomeric DNA is expected to form a hybrid-type mixed parallel/antiparallel-stranded G-quadruplex in the presence of K^+ [7-9].

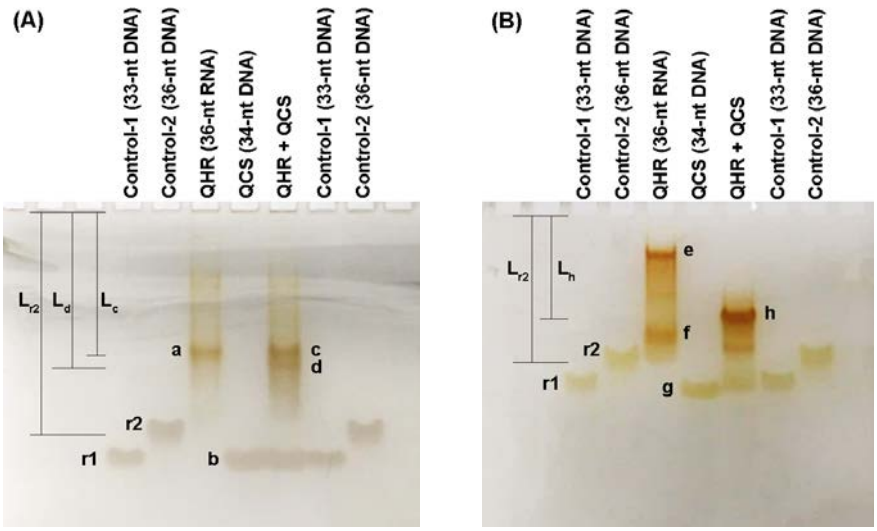

Fig. S3. Native PAGE analysis of QHR-QCS system. Native PAGE in the presence (A) and absence (B) of 100 mM KCl. L_{r2}, L_c, L_d and L_h indicate the mobility of bands, **r2**, **c**, **d** and **h**, respectively, in each gel.

QHR (36-nt RNA), QCS (34-nt DNA), a mixture of QHR and QCS, two control DNAs that are supposed not to form a particular structure, Control-1 (33-nt DNA, d(CGCGGATCCCGAGCTGGTGACTGGAAGTGTCCT)) and Control-2 (36-nt DNA, d(GATCTCTAGAATCTGGTTTAGGGGCCTTACACTGGT)), were applied to the native PAGE. Each sample dissolved in ca. 62 mM Tris-HCl buffer (pH 8.0) was incubated at 95 °C for 5 min, then cooled to 30 °C in 60 min, and incubated at 25 °C for 30 min. Each sample (4 μM) dissolved in 50 mM Tris-HCl buffer (pH 8.0), 10 mM $MgCl_2$, and either 0 or 100 mM KCl was incubated at 25 °C for 60 min, and run on the native PAGE.

In the presence of 100 mM KCl, the mobility of QHR (36-nt, band **a**) was much lower than that of Control-2 (36-nt, band **r2**) (Fig. S3A), which suggests that QHR formed a dimer of the quadruplex (36-nt + 36-nt). In the presence of 100 mM KCl, two bands, **c** and **d**, were found for a mixture of QHR and QCS (Fig. S3A). The mobility of the main band **c** coincides with that of the band **a** observed for QHR. This indicates that in the presence of 100 mM KCl, QHR forms the dimer of the quadruplex even under the co-existence of QCS. The mobility of the minor band **d** is slightly higher than that of the main band **c**, which suggests that the band **d** corresponds to the QHR-QCS duplex (36-nt + 34-nt).

In the absence of KCl, a main band **h** was found for a mixture of QHR and QCS (Fig. S3B). In order to compare the mobility in two gels, relative mobility was defined as equation (1) for each gel:

relative mobility = mobility of each band (either L_c, L_d or L_h) / mobility of Control-2 (L_{r2}) (1)

The relative mobility of the bands **c** and **d** were 0.65 and 0.70, respectively. The relative mobility of

the band **h** was 0.70. This indicates that the main band **h** corresponds to the QHR-QCS duplex. That is, in the absence of KCl, the QHR-QCS duplex was mainly formed for the mixture of QHR and QCS.

In summary, when QCS co-existed, QHR mainly formed the QHR-QCS duplex in the absence of KCl, while it mainly formed the dimer of the quadruplex in the presence of 100 mM KCl. Thus, the native PAGE analysis also supports the conformational change concluded from NMR and CD analyses.

QCS is expected to form the quadruplex structure in the presence of 100 mM KCl. The mobility of QCS is not so different between in the presence and absence of 100 mM KCl (Fig. S3A and B). The mobility of the quadruplex structure depends on its shape, so it is hard to deduce the formation of the quadruplex solely from PAGE analysis. Instead, the formation of the quadruplex for QCS is clearly revealed by NMR analysis (Fig. S4). Appearance of imino proton resonances around at 10.5 - 12.2 ppm indicates the formation of the quadruplex for QCS in the presence of 100 mM KCl, as expected.

Low mobility band **e** was found for QHR only in the absence of 100 mM KCl (Fig. S3B). It was reported that d(GGAGGAN) forms a unique parallel duplex with mismatch-aligned arrowhead motifs only under low salt conditions [10]. Band **e** may be an oligomer related to this structure, although decisive identification of the structure is not feasible.

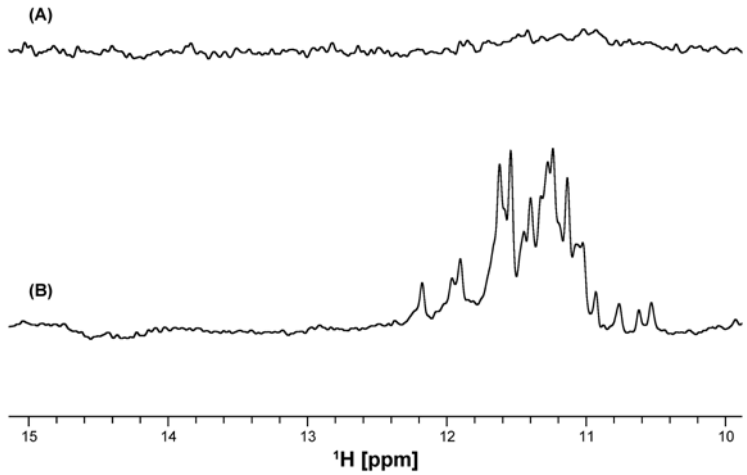

Fig. S4. NMR analysis of QCS. QCS (70 μM) was dissolved in 5 mM sodium phosphate buffer (pH 6.5) containing 5 mM $MgCl_2$, and either 0 mM (A) or 100 mM (B) KCl at 25 °C. Appearance of imino proton resonances around at 10.5 - 12.2 ppm (B) indicates the formation of the quadruplex for QCS in the presence of 100 mM KCl.

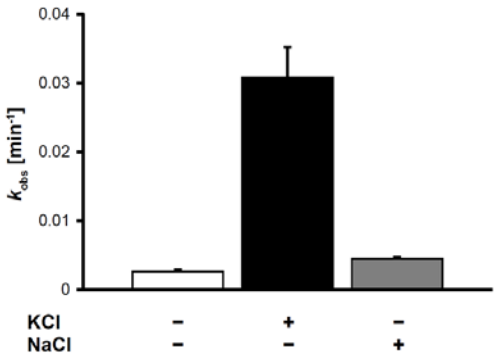

Fig. S5. The effect of Na^+ on the activity of the QHR-QCS system. The first-order rate constants of the cleavage reaction with the QHR-QCS system, composed of QHR and QCS, were obtained for the reaction performed either in the absence of K^+ and Na^+ (open box), in the presence of 100 mM K^+ (black box), or in the presence of 100 mM Na^+ (gray box).

References

[1] A.N. Lane, J.B. Chaires, R.D. Gray, J.O. Trent, Stability and kinetics of G-quadruplex structures, Nucleic Acids Res. 36 (2008) 5482-5515.

[2] S. Paramasivan, I. Rujan, P.H. Bolton, Circular dichroism of quadruplex DNAs: applications to structure, cation effects and ligand binding, Methods 43 (2007) 324-331.

[3] T. Mashima, A. Matsugami, F. Nishikawa, S. Nishikawa, M. Katahira, Unique quadruplex structure and interaction of an RNA aptamer against bovine prion protein, Nucleic Acids Res. 37 (2009) 6249-6258.

[4] T. Mashima, F. Nishikawa, Y.O. Kamatari, H. Fujiwara, M. Saimura, T. Nagata, T. Kodaki, S. Nishikawa, K. Kuwata, M. Katahira, Anti-prion activity of an RNA aptamer and its structural basis, Nucleic Acids Res. 41 (2013) 1355-1362.

[5] D. Renciuk, I. Kejnovská, P. Skoláková, K. Bednárová, J. Motlová, M. Vorlícková, Arrangements of human telomere DNA quadruplex in physiologically relevant K^+ solutions, Nucleic Acids Res. 37 (2009) 6625-6634.

[6] Y. Xu, Y. Noguchi, H. Sugiyama, The new models of the human telomere d[AGGG(TTAGGG)3] in K^+ solution, Bioorg. Med. Chem. 14 (2006) 5584-5591.

[7] J. Dai, M. Carver, C. Punchihewa, R.A. Jones, D. Yang, Structure of the Hybrid-2 type intramolecular human telomeric G-quadruplex in K^+ solution: insights into structure polymorphism of the human telomeric sequence, Nucleic Acids Res. 35 (2007) 4927-4940.

[8] K.N. Luu, A.T. Phan, V. Kuryavyi, L. Lacroix, D.J. Patel, Structure of the human telomere in K^+ solution: an intramolecular (3 + 1) G-quadruplex scaffold, J. Am. Chem. Soc. 128 (2006) 9963-9970.

[9] A. Matsugami, Y. Xu, Y. Noguchi, H. Sugiyama, M. Katahira, Structure of a human telomeric DNA sequence stabilized by 8-bromoguanosine substitutions, as determined by NMR in a K^+ solution, FEBS J. 274 (2007) 3545-3556.

[10] A. Kettani, A. S. Bouaziz, E. Skripkin, A. Majumdar, W. Wang, R. Jones, D.J. Patel, Interlocked mismatch-aligned arrowhead DNA motifs, Structure 7 (1999) 803-815.